

# Pairing Glue Activation in Cuprates within the Quantum Critical Regime

Josef Ashkenazi and Neil F. Johnson

*Physics Department, University of Miami, P.O. Box 248046, Coral Gables, FL 33126, U.S.A.*

(Dated: May 31, 2022)

A grand challenge in many-body quantum physics is to explain the apparent connection between quantum criticality and high-temperature superconductivity in the cuprates. We argue that a quantum-critical regime plays an essential role in activating a strong-pairing mechanism: although pairing bosons create a symmetry-breaking instability which suppresses pairing, the combination of these broken-symmetry states *restores* this symmetry for the paired quasiparticles. A hidden quantum phase transition then arises between a Fermi-liquid and a non-Fermi-liquid broken-symmetry striped state, and a critical regime in which the broken-symmetry states are combined. A general prediction of our theory is that a similar pairing scenario will arise in any superconducting system with a quantum critical regime, e.g. the iron pnictides and chalcogenides.

PACS numbers: 74.40.Kb, 74.72.-h, 74.25.Dw, 74.20.Mn

A major obstacle in the efforts to raise the superconducting (SC) transition temperature  $T_c$  in electron-phonon systems has been the emergence of symmetry-breaking structural instabilities [1] when the electron-phonon coupling constants become too strong. These instabilities open gaps on the Fermi surface (FS), thereby reducing the magnitude of the pairing-strength parameter [2]  $\lambda$  and preventing possible increases in  $T_c$ . This is also one of the reasons why non-phonon mechanisms were offered as an explanation of high- $T_c$  superconductivity (HTSC) in the cuprates. However such mechanisms generally suffer from a similar problem, i.e., competition between pairing and symmetry-breaking instabilities of spin or charge inhomogeneity. The breakdown of time-reversal symmetry (in the case of a magnetic inhomogeneity) introduces a further limitation to HTSC [3, 4].

A wide class of SC systems such as high- $T_c$  cuprates, Fe-based superconductors (FeSCs), organic and other SC systems, are characterized by anomalous features which are inconsistent with normal Fermi-liquid (FL) behavior. One major anomalous feature is the *linear* dependence of the scattering rates on temperature ( $T$ ) or energy ( $\omega$ ), which has been suggested [5] as characterizing a non-FL state, known as the “marginal FL” (MFL) state. This state has been attributed to quantum criticality [6–9] within the critical regime of a quantum phase transition at  $T = 0$ . Such quantum criticality occurs in magnetic insulators [8], e.g.,  $\text{TiCuCl}_3$  under pressure [10]. At low pressures (i.e. system-variation parameter  $g > g_c$ ), the ground state of this system is a dimerized antiferromagnet (AF) with neighboring spins forming singlet pairs, and the excitations are “triplons” (i.e. triplet excitations of singlet dimers). At high pressures (i.e.  $g < g_c$ ), the ground state is a Néel AF and the excitations are spin waves. This latter state exists only at  $T = 0$  and breaks the symmetry between different possible spin arrangements, as well as the spin rotation symmetry. Within either the  $g < g_c$  or the  $g > g_c$  regimes, a reasonable description of the quantum state at low temperatures

[8] could be based on a mixture of a few low-energy excited states. By contrast at the quantum critical point  $(g, T) = (g_c, 0)$ , the quantum state is a combination of states with macroscopically different symmetries, resulting in highly nontrivial behavior. Such a behavior persists [8] at  $T > 0$  within the quantum critical regime. This regime could be referred to as a quantum critical state, but its boundaries are not sharp and instead represent gradual (i.e. not phase) transitions for  $T > 0$ . Such a phase diagram resembles that of the cuprates (and similar SC systems) [8] when the SC regime is suppressed. In this comparison  $g$  represents the doping level, the quantum critical regime corresponds to the MFL state, and the regimes of lower and higher doping levels correspond to the pseudogap (PG) and FL states, respectively. It has been suggested [11] that quantum criticality in high- $T_c$  systems gives rise to a “critical glue” which provides SC pairing – however its identity is so far unknown. More generally, there have been many attempts to interpret quantum criticality in condensed matter systems using insights from other domains [8, 9, 11–14].

Here we develop a theory focusing on hole-doped cuprates [15, 16] although our theory’s conclusions are expected to apply to a far wider class of SC systems. The minimal reduced Hamiltonian necessary to study the major low-energy features of the cuprates is [16] a one-band 2D Hubbard model on a square lattice (unit vectors  $a\hat{x}$  and  $a\hat{y}$ ), with transfer integrals up to the third-nearest neighbor (i.e. including  $t$ ,  $t'$  and  $t''$ ). The on-site Coulomb repulsion parameter  $U$  within this band corresponds to the large-to-intermediate- $U$  regime. We note that a dynamical cluster quantum Monte Carlo study of the 2D Hubbard model [17, 18] confirmed the existence of a MFL regime, between PG and FL regimes, in the normal state. A related attempt [19] to prove that the calculated  $T_c$  is raised within the quantum critical (MFL) regime, was less conclusive [18]. Since it was based on electron-like quasiparticles (QPs) which are paired due to their coupling to spin fluctuations, and such QPs cor-

respond to a FL state, it is doubtful whether a pairing theory in a non-FL state could be based on them. By contrast, QPs appropriate for large- $U$  systems can be determined using the auxiliary-particle approach [20], and this should also provide a reasonable description in the intermediate- $U$  regime. Auxiliary particles can be described [15] as combinations of atomic-like configurations with the same number of electrons per site. Hence beside the cuprates, this approach is also applicable to low-energy excitations in multi-band systems such as the FeSCs [15].

Since there can only be one configuration in a given site at a given time, the auxiliary particles must fulfill the constraint under which the sum of their numbers at *any* site is 1. In the large  $U$  limit, the auxiliary particles corresponding to the same number of electrons per site can be chosen to be either all bosons or all fermions [15]. Those corresponding to one electron more, or less, per site are of the opposite type (i.e. fermions if the others are bosons, or *vice versa*). Since condensates of boson auxiliary particles play a significant role in the present theory [15, 16] (see below), we refer to it as the auxiliary Bose condensates (ABC) approach. We choose auxiliary particles corresponding to the number of electrons per site characterizing the undoped stoichiometry (thus the parent compound) to be bosons [15] and refer to them as svivons. Auxiliary particles corresponding to hole- or electron-doped sites are thus fermions, referred to as quasi-electrons (QEs). The QPs which carry charge (due to doping) are hence fermions, while the spin, orbital and charge ordering are each associated with bosons and their condensation. In the cuprates, this choice corresponds to the slave fermion, as opposed to the slave boson method (including the Gutzwiller approximation) which characterizes most RVB models. Due to the presence of dynamical inhomogeneities, the number constraint is maintained within the ABC approach in a site-dependent and time-dependent manner [15]. A dynamical field of Lagrange multipliers is introduced which is equivalent to a field of bosons, referred to as lagrons [16]. Within a grand-canonical scheme, the Hamiltonian includes [15, 16] QE-lagron and svivon-lagron coupling terms. Due to the nature of the constraint, they represent the coupling of electrons to spin, orbital and charge fluctuations.

Studies [21] using similar Hamiltonians predict that the interplay between electron hopping and AF exchange in the cuprates can drive the formation of the empirically observed striped structures [22, 23], characterized by a spin density wave (SDW) with wave vector:

$$\mathbf{Q}_m = \mathbf{Q} + \delta\mathbf{q}_m, \text{ for } m = 1 \text{ or } 2 \text{ or } 3 \text{ or } 4, \quad (1)$$

where  $\mathbf{Q} = (\pi/a)(\hat{x} + \hat{y})$  is the wave vector of the AF order in the parent compounds, and  $\delta\mathbf{q}_m = \pm\delta q\hat{x}$  or  $\pm\delta q\hat{y}$  are modulations around  $\mathbf{Q}$ . Typically  $\delta q \cong \pi/4a$ , and the SDW is accompanied by a charge density wave of wave vector  $2\delta\mathbf{q}_m$  [22, 23]. Similarly to the Néel state

in [8, 10]  $\text{TlCuCl}_3$ , these striped states break the symmetry between different possible spin arrangements and under spin rotations. Within the ABC approach, they correspond [16] to a Bose-condensed svivon field whose spectrum has a V-shape energy minimum  $k_B T/\mathcal{O}(N)$  at the points  $\pm\mathbf{Q}_m/2$ . Consequently, gaps open on a part of the QE and electron FS [16], similarly to the case of structural instabilities [1]. Time-reversal symmetry is also removed, as happens in a SDW [3, 4]. Both effects counter the establishment of a SC state.

However, it was shown [16] that a combination state of different svivon Bose condensates, corresponding to symmetry-breaking striped states, can yield HTSC. In this state each condensate is not an eigenstate; consequently [15, 16] the energy minima of the svivon spectrum rise above zero and become parabolic. The combination state is generated [16] by a lagron spectrum with V-shape minima of energy  $k_B T/\mathcal{O}(N)$  at the four  $\mathbf{Q}_m$  points in Eq. (1). Thus the lagron Bose field is also condensed [16]. Electron states are convoluted QE-svivon states [15, 16], hence the electron Green's functions are dressed bubble diagrams of QE and svivon Green's functions. The major dressing effect for unpaired electrons is due to multiple scattering of QE-svivon pairs through inter-site transfer, resulting in the introduction of a pole. Consequently, the normal-state electron Green's functions have two types of poles [16]: (i) QE-svivon convolution introduces a continuity of poles per  $\mathbf{k}$  state, with maximal contribution from svivons close to their energy minima, and thus a non-FL-type feature; (ii) the multiple-scattering dressing effect introduces one pole per  $\mathbf{k}$  state, and thus a FL-type feature. The quantum state of normal-state electrons is therefore a combination of a FL state and non-FL states of different broken-symmetry striped structures. This combination state is characteristic of a quantum critical regime [8] even though this aspect was not considered in the original derivation [15, 16]. Indeed the observed critical regime appears projected from a  $T = 0$  quantum phase transition which is missing due to the SC regime. This hidden transition is between a low-doping broken-symmetry non-FL striped state, and a high-doping symmetry-maintaining FL state.

Since the broken-symmetry striped states correspond to svivon condensates, their combination restores symmetry *vis a vis* the QEs. The evaluation of their spectrum, and also that of the electron, is based on an adiabatic treatment of the combined striped structures. The resulting QE spectrum [16] includes the AF wave vector  $\mathbf{Q}$  as a reciprocal lattice vector, due to averaging over points  $\mathbf{Q}_m$  in Eq. (1). This is reflected in the existence of equivalent main and shadow QE bands. The equivalence between these bands is removed in the resulting electron spectrum [16], but still both exist. Signatures of the  $\mathbf{Q}_m$  wave vectors are expected to persist in cases of slow stripes dynamics. Areas of flat, polaron-like, low-energy QE bands also arise in the Brillouin zone (BZ).

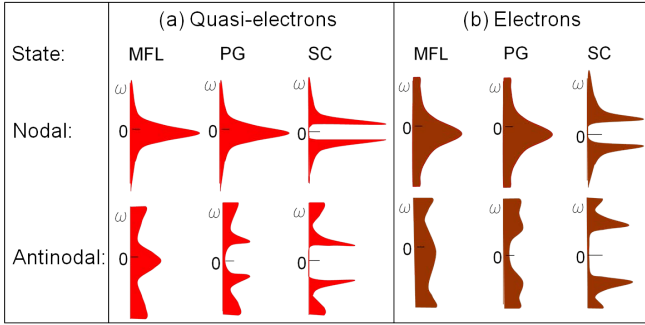


FIG. 1: Typical low-energy (a) QE and (b) electron spectral functions in the MFL, PG and SC states, at nodal and antinodal points in hole-doped cuprates. The antinodal QEs are paired both in the PG and the SC states, while nodal QEs are paired only in the SC state.

There is an abrupt transition between these bands and the higher-energy QE bands in the rest of the BZ. This feature is reflected in the electron bands through the existence of kinks close the Fermi level ( $E_F$ ) followed by “waterfalls” further away from  $E_F$ . The QE spectral functions within the low-energy BZ areas reflect the effect of the fluctuating stripes. For a static striped state (i.e. a SDW) of one of the  $\mathbf{Q}_m$  wave vectors in Eq. (1), a gap around zero energy opens up at low  $T$ , in  $\mathbf{k}$  points of low-energy QEs, if there are low energy QEs close to  $\mathbf{k} + \mathbf{Q}_m$  or  $\mathbf{k} - \mathbf{Q}_m$ . This results in a split-peak QE spectral structure near such  $\mathbf{k}$  points, and a one-peak QE spectral structure at other low-energy  $\mathbf{k}$  points.

The quantum-critical state is now a combination of striped states at the different  $\mathbf{Q}_m$  wave vectors in Eq. (1). Consequently, there are low-QE-energy  $\mathbf{k}$  points close to the antinodal BZ areas, where the split-peak and one-peak scenarios are combined, while at the other  $\mathbf{k}$  points close to the nodal BZ areas, the single-peak scenario prevails. These spectral features of the low-energy QEs are sketched in Fig. 1(a). Since each peak in the spectral functions corresponds to a pole in the QE Green’s functions, the QE BZ is divided into two analytically distinct  $T$ -dependent areas. The Green’s functions have one pole per  $\mathbf{k}$  point in one area, and three poles in the other. Figure 1(b) shows schematically the reflection of these features in the non-FL part of the electron spectral function close to  $E_F$ . The results for the electron scattering rates  $\Gamma^d(\mathbf{k}, \omega, T)$  are presented in Fig. 2. For small and intermediate values of  $\omega$  and  $T$ , these results are dominated by terms of the form:

$$\Gamma^d(\mathbf{k}, \omega, T) \simeq \Gamma_0^d(\mathbf{k}) - \Gamma_1^d(\mathbf{k})|\omega|b_T(-|\omega|), \quad (2)$$

where  $b_T(\omega) \equiv 1/[\exp(\omega/k_B T) - 1]$  is the Bose distribution function. Eq. (2) yields:

$$\Gamma^d(\mathbf{k}, \omega, T) \simeq \begin{cases} \Gamma_0^d(\mathbf{k}) + \Gamma_1^d(\mathbf{k})k_B T, & \text{for } |\omega| \ll k_B T, \\ \Gamma_0^d(\mathbf{k}) + \Gamma_1^d(\mathbf{k})|\omega|, & \text{for } |\omega| \gg k_B T, \end{cases} \quad (3)$$

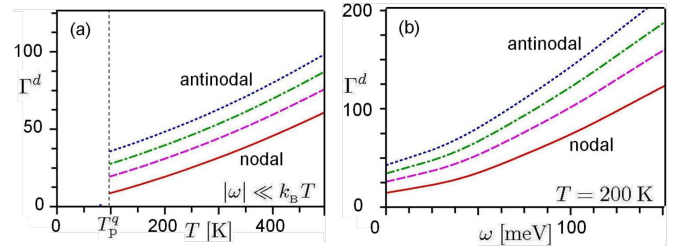


FIG. 2: Typical trends for (a) the  $T$  dependence, and (b) the  $\omega$  dependence of the electron scattering rates  $\Gamma^d$ , within the MFL regime (i.e.  $T$  above the QE pairing temperature  $T_p^q$ ) at  $\mathbf{k}$  points ranging between the nodal and antinodal parts of the FS.

in agreement with MFL phenomenology [5]. This further confirms that our description is realistic for a quantum critical state.

The linear variation of  $\Gamma^d(\mathbf{k}, \omega, T)$  with  $\omega$  and  $T$ , is driven from the QE-sivion convolution expression. The strong scattering processes determining it are mostly due to the coupling of the auxiliary particles to lagrons. This coupling also induces QE pairing, under which the electrons become paired as well. Note that coupling of QEs through lagrons results in the striped states, but this coupling causes pairing only in the combination of striped states due to quantum criticality. Hence the lagrons are playing the role of a *critical pairing glue* which is activated in the critical regime. This glue is deactivated for static striped states, and fades away within the FL regime. Since the BZ of the low-energy QEs is divided into two analytically distinct parts, pairing can occur below different temperatures,  $T^*$  ( $T^* > T_c$ ) and  $T_c$  in the antinodal and nodal areas respectively. SC occurs for  $T < T_c$ , while PG occurs for  $T_c < T < T^*$ . Figure 1 illustrates the effect of pairing on the low-energy QE spectral structure in the PG and in the SC states, and on the electron spectral function close to  $E_F$ .

The pairing-strength parameter  $\lambda$ , due to QE-lagron coupling in the hole-doped cuprates, is estimated [16] to be  $\lambda \simeq 3$ . Such large values explain [2] the enhancement of  $T_c$  compared to conventional electron-phonon superconductors, where large values of  $\lambda$  are prevented due to the occurrence of lattice instabilities for strong electron-phonon coupling [1]. Instabilities due to QE-lagron coupling do occur but are combined within the quantum critical regime, hence enabling these large  $\lambda$  values to occur. Partial pairing around the antinodal BZ areas does occur in the PG state, but does not result in Cooper pairs which can carry supercurrent (due to scattering between different  $(\mathbf{k}, -\mathbf{k})$  states without breaking). However in the PG state, QE pairs are broken due to scattering between the antinodal and the nodal BZ areas. There is mounting evidence that a regime of SC fluctuations generally exists in the cuprates above  $T_c$ , depending on disorder *etc.*, but that it does not correspond to the PG

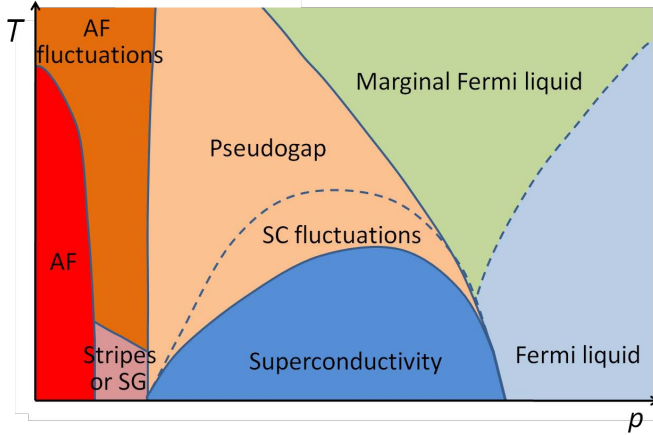


FIG. 3: Our proposed phase diagram for the hole-doped cuprates, under changing temperature and doping level  $p$ . Solid and dashed lines represent phase and gradual transitions, respectively.

state [24, 25]. For  $T > T^*$ , the stripe dynamics are fast, and the short lifetimes of the striped structures yields features which are too broad to be observed experimentally. This changes when at least a partial gap opens up in the PG and the SC states [16]. Indeed, the existence of fluctuating stripes has been observed for  $T < T^*$  using STM [26], and the resulting broken rotational symmetry through the anisotropic Nernst effect [27]. The behavior of the fluctuating stripes has been analyzed by analogy to nematicity in liquid crystals [30, 31]. The existence of fluctuating striped structures (Eq. (1)) implies that experiments measuring timescales shorter than the stripe dynamics will detect violations of time-reversal symmetry, while longer timescale experiments will not. Neutron scattering measurements [28] indicate such violation for  $T < T^*$ , while Zeeman-perturbed NQR results [29] do not indicate it. The existence of static time-reversal symmetry means that the negative effect of its absence on pairing in a striped state [3, 4] is absent when the stripes are fluctuating.

The energy gain due to the establishment of the PG and SC states, which arise from a combination of striped states, actually extends the range where the critical regime exists beyond typical critical regimes in magnetic insulators such as [8, 10]  $\text{TlCuCl}_3$ , into the PG and SC regimes. The resulting phase diagram of the hole-doped cuprates is sketched in Fig. 3. Unlike in magnetic insulators, this phase diagram does not include a quantum critical point, unless pairing is suppressed down to  $T = 0$ . The MFL regime is reminiscent of the high- $T$  part of the quantum critical regime in magnetic insulators [8, 10], and so is the gradual transition between the MFL and the FL regimes. It is manifested as a crossover between the linear behavior of the scattering rates (Fig. 2) and a quadratic behavior characteristic of a FL. Typically for a gradual transition, remnants of MFL behavior persist

within the normal state of the overdoped regime [32]. By contrast, the boundary between the MFL and the PG regimes is characterized by a phase transition, and our theory predicts that a phase transition also occurs between the PG state and the states for lower doping levels (Fig. 3).

Similar predictions follow for other SC systems which include a quantum-critical regime. The key feature is that the pairing bosons – which could be of a similar, or a different, nature compared to the ones in the cuprates – introduce a symmetry-breaking instability, and these broken-symmetry states are combined in the critical regime, restoring symmetry for the paired QPs. Similar QPs and pairing bosons to those in the cuprates, are expected for the FeSCs, though they will be more evolved due to their multi-band nature. Our theory also predicts that the quantum phase transition in the FeSCs is between a non-FL magnetic state and a FL state, and the broken-symmetry states are the perpendicular-direction SDWs [33] which exist, or almost exist, in the magnetic state.

- 
- [1] L. R. Testardi, *Rev. Mod. Phys.* **47**, 637 (1975).
  - [2] V. Z. Kresin, and S. A. Wolf, *Rev. Mod. Phys.* **81**, 481 (2009).
  - [3] J. Ashkenazi, C. G. Kuper, and A. Ron, *Phys. Rev. B* **28**, 418 (1983).
  - [4] J. Ashkenazi, C. G. Kuper, M. Revzen, A. Ron, and D. Schmeltzer, *Solid State Commun.* **51**, 135 (1984).
  - [5] C. M. Varma, P. B. Littlewood, S. Schmitt-Rink, E. Abrahams and A. E. Ruckenstein, *Phys. Rev. Lett.* **63**, 1996 (1989).
  - [6] C. Castellani, C. Di Castro, and M. Grilli, *Physica C* **282–287**, 260 (1997).
  - [7] Y. Dagan and G. Deutscher, *Phys. Rev. Lett.* **87**, 177004 (2001).
  - [8] Subir Sachdev and Bernhard Keimer, *Physics Today* **64**, 29 (2011), and references therein.
  - [9] Jan Zaanen, in *100 years of superconductivity*, edited by H. Rogalla and P. H. Kes (Taylor & Francis, 2011), arXiv:1012.5461.
  - [10] Ch. Rüegg, B. Normand, M. Matsumoto, A. Furrer, D. F. McMorrow, K. W. Krämer, H.-U. Güdel, S. N. Gvasaliya, H. Mutka, and M. Boehm, *Phys. Rev. Lett.* **100**, 205701 (2008).
  - [11] J.-H. She, B. J. Overbosch, Y.-W. Sun, Y. Liu, K. Schalm, J. A. Mydosh, and J. Zaanen, *Phys. Rev. B* **84**, 144527 (2011).
  - [12] Subir Sachdev, arXiv:1108.1197.
  - [13] M. Edalati, R. G. Leigh, K. W. Lo, and P. W. Phillips, *Phys. Rev. D* **83**, 045012 (2011).
  - [14] W. H. Zurek, *Nature* **317**, 505 (1985).
  - [15] J. Ashkenazi, *J. Supercond. Nov. Magn.* **22**, 3 (2009).
  - [16] J. Ashkenazi, *J. Supercond. Nov. Mag.* **24**, 1281 (2011).
  - [17] N. S. Vidhyadhiraja, A. Macridin, C. Sen, M. Jarrell, and M. Ma, *Phys. Rev. Lett.* **102**, 206407 (2009).
  - [18] K.-S. Chen, S. Pathak, S.-X. Yang, S.-Q. Su,

- D. Galanakis, K. Mikelsons, M. Jarrell, and J. Moreno, arXiv:1104.3261.
- [19] S.-X. Yang, H. Fotso, S.-Q. Su, D. Galanakis, E. Khatami, J.-H. She, J. Moreno, J. Zaanen, and M. Jarrell, *Phys. Rev. Lett.* **106**, 047004 (2011).
- [20] S. E. Barnes, *Adv. Phys.* **30**, 801 (1981).
- [21] V. J. Emery, and S. A. Kivelson, *Physica C* **209**, 597 (1993).
- [22] J. M. Tranquada, J. D. Axe, N. Ichikawa, Y. Nakamura, S. Uchida, and B. Nachumi, *Phys. Rev. B* **54**, 7489 (1996).
- [23] M. Fujita, H. Goka, K. Yamada, J. M. Tranquada, and L. P. Regnault, *Phys. Rev. B* **70**, 104517 (2004).
- [24] H. Alloul, F. Rullier-Albenque, B. Vignolle, D. Colson, and A. Forget, *Europhys. Lett.* **91**, 37005 (2010).
- [25] N. F. Johnson, J. Ashkenazi, Z. Zhao, and L. Quiroga, *AIP Advances* **1**, 012114 (2011), and references therein.
- [26] C. V. Parker, P. Aynajian, E. H. da Silva Neto, A. Pushp, S. Ono, J. Wen, Z. Xu, G. Gu, and A. Yazdani, *Nature* **468**, 677 (2010).
- [27] R. Daou, J. Chang, D. LeBoeuf, O. Cyr-Choinière, F. Laliberté, N. Doiron-Leyraud, B. J. Ramshaw, R. Liang, D. A. Bonn, W. N. Hardy, and L. Taillefer, *Nature* **463**, 519 (2010).
- [28] Y. Li, V. Balédent, G. Yu, N. Barisić, K. Hradil, R. A. Mole, Y. Sidis, P. Steffens, X. Zhao, P. Bourges, and M. Greven, *Nature* **468**, 283 (2010).
- [29] S. Strässle, B. Graneli, M. Mali, J. Roos1, and H. Keller, *Phys. Rev. Lett.* **106**, 097003 (2011).
- [30] S. A. Kivelson, E. Fradkin, and V. J. Emery, *Nature* **393**, 560 (1998).
- [31] M. J. Lawler, K. Fujita, J. Lee, A. R. Schmidt, Y. Kohsaka, C.-K. Kim, H. Eisaki, S. Uchida, J. C. Davis, J. P. Sethna, and E.-A. Kim, *Nature* **466**, 347 (2010).
- [32] J. Kokalj and R. H. McKenzie, *Phys. Rev. Lett.* **107**, 147001 (2011).
- [33] C. de la Cruz, Q. Huang, J. W. Lynn, J. Li, W. Ratcliff II, J. L. Zarestky, H. A. Mook, G. F. Chen, J. L. Luo, N. L. Wang, and Pengcheng Dai, *Nature* **453**, 899 (2008).